



# Carbon dots-enhanced pH-responsive lubricating hydrogel based on reversible dynamic covalent bondings

Jianye Kang<sup>a</sup>, Xinyu Yang<sup>a</sup>, Xuhao Yang<sup>a</sup>, Jiahui Sun<sup>a</sup>, Yuhang Liu<sup>a</sup>, Shutao Wang<sup>b,c</sup>, Wenlong Song<sup>a,\*</sup>

<sup>a</sup> State Key Laboratory of Supramolecular Structure and Materials, College of Chemistry, Jilin University, Changchun 130012, China

<sup>b</sup> CAS Key Laboratory of Bio-inspired Materials and Interfacial Science, CAS Center for Excellence in Nanoscience, Technical Institute of Physics and Chemistry, Chinese Academy of Sciences, Beijing 100190, China

<sup>c</sup> University of Chinese Academy of Sciences, Beijing 100049, China

## ARTICLE INFO

### Article history:

Received 19 September 2023

Revised 7 November 2023

Accepted 8 November 2023

Available online 11 November 2023

### Keywords:

pH-responsive

Carbon dots

Dynamic covalent bonding

Lubrication

## ABSTRACT

Due to the various pH liquid environment in nature, the pH-responsive lubricating hydrogel is widely investigated and developed for tissue interface substitute. However, the applied liquid environment will lead to poor mechanical property and weaken the pH-responsive capability. In this work, a carbon dots-enhanced pH-responsive lubricating hydrogel is developed by combining a pH-responsive section of dynamic PVA-borax network into a PAAm covalent polymer network. The formed hydrogel presents a partial gel-sol transition under controlled pH environments. At low pH environments (<6.0), the formed lubricating layer originated from dynamic disassembly of PVA-borax hydrogel, and brings the lubricating properties on the hydrogel surface. Moreover, the mechanical strength and lubrication properties are well promoted by introducing the carbon dots into the hydrogel, the blue sol layer can be observed more visually under the fluorescence microscope. The pH-response also exhibits well reversibility. The prepared hydrogel broadens the idea for designing pH-responsive soft materials for soft lubricating actuator or robot.

© 2024 Published by Elsevier B.V. on behalf of Chinese Chemical Society and Institute of Materia Medica, Chinese Academy of Medical Sciences.

Smart hydrogel that can feedback the external stimuli (such as pH, temperature, electricity, light, ionic strength, shear force) has been widely developed for their promising potential in biomedicine [1,2], shape memory hydrogels [3,4], self-healing [5,6], soft wearable devices [7,8] and actuators [9,10]. Among these stimuli, pH-responsive hydrogel is investigated widely [11–14], because the liquid environment in human body varies greatly. For example, the blood and cellular fluid of muscle and skin are nearly neutral at pH 6.0–7.4; the gastric mucosa is extremely acidic at pH 1.0–3.5; the bile and pancreatic fluid are alkaline at pH 7.6–8.8 [15]. As a result, the physiological function of these tissues is also affected by pH, such as lubrication, anti-virus, nutrient transport, and biological signal communication. The pH-responsive hydrogel is developed for satisfying the requirement in artificial tissue, biomedicine or soft actuator. For example, by utilizing the pH-response on the protonation state of polyacrylic acid, the lubrication on poly(acrylamide-co-acrylic acid) hydrogel was managed to superlubricity level (~0.005) [16]. Moreover, a pH-responsive

DNA hydrogel composed of adenine-rich and cytosine-rich oligonucleotides and polyacrylamide (PAAm) was fabricated as carrier for insulin encapsulation and oral delivery in acidic condition (pH 1.2–6.0) [17]. The drug could be released following the process of gel-sol transition at physiological pH 7.2, which was attributed to the disassembly of the two cross-linking units to single-stranded adenine-rich and cytosine-rich sequences. As the sol appearance after the gel-sol transition, it might be utilized to regulate the lubrication on the hydrogel surface.

Generally, the gel-sol transition capability of hydrogel includes two network system: the supramolecular noncovalent bonding network and the dynamic covalent bondings network. Through the strategy on combining supramolecular network into covalent network a semi-convertible hydrogel was prepared that exhibited responsive lubrication capability due to the gel-sol transition partly [18–20]. Besides the supramolecular gel-sol transition system, the esterification of boronic acid with polyvinyl alcohol (PVA-borax) is a typical dynamic covalent bonding system leading to reversible formation of boronic ester following the pH change [21–23]. When pH decreases below the  $pK_a$  [24–26] of the boronic acids, the hydrogel transforms to sol state due to the broken of the borate es-

\* Corresponding author.

E-mail address: [songwenlong@jlu.edu.cn](mailto:songwenlong@jlu.edu.cn) (W. Song).

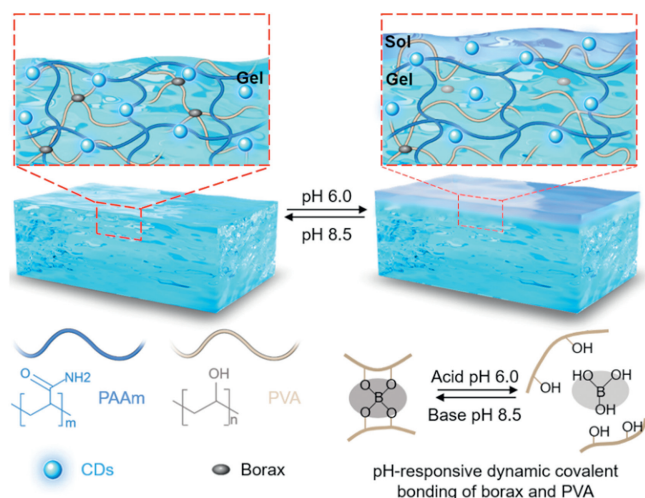


**Fig. 1.** The lubricating mechanism of the CDs-enhanced pH-responsive lubricating hydrogel, and composition of the prepared hydrogel.

ter bonding. When the pH increases higher than the  $pK_a$ , the borate ester bonding is re-formed, and the PVA-borax sol transforms into gel state. If the dynamic covalent bonding system is embedded into another polymer network, the proposed hydrogel might exhibit both pH-response lubricating character and stable framework. However, the pH-responsive liquid environment would weaken the mechanical property due to the swelling behavior of the hydrogel. The doping strategy of particles is thought to be a possible way for overcoming this limitation. Carbon dots (CDs) is a new kind of carbon nanomaterials [27–29], which exhibits various fluorescent properties, biocompatible and non-toxicity [30–36]. It is widely used in lubricants [37–39], catalysis [40–45], bioimaging [46–50], medical therapeutics [51–53], and antibacterial [54–57]. If CDs was doped in the pH-responsive lubricating hydrogel network, the lubrication and mechanics might be improved due to its appearance on the hydrogel surface accompanied by the gel-sol transition process. Meanwhile, CDs composite would also increase the possibility of improving the mechanical properties of hydrogels. Herein, a CDs-enhanced pH-responsive lubricating hydrogel (CPLH) was fabricated composing of PVA-borax, PAAm and CDs (Fig. 1). The hydrogel will occur partly gel-sol transition corresponding to the  $pK_a$  of boronic acid while the whole hydrogel keeps gel state due to the existence of PAAm covalent frameworks. The sol state PVA with boronic acid and free CDs appears on the hydrogel surface that the responsive lubricating property might be achieved and further improved due to the introduction of CDs. Correspondingly the mechanics of the prepared hydrogel will also be tuned following the pH changes.

As described in Fig. 1, the pH responsiveness of the prepared hydrogel is derived from the dynamic borate ester bond of PVA-borax, which brings the gel-sol transition of PVA-borax hydrogel under different pH. When it was treated by the solution with pH range from 1.0 to 6.0, the gel-sol transition can be observed (Fig. S1a in Supporting information). When pH further increased higher than 8.0, no gel-sol transition occurred on the hydrogel. The storage modulus ( $G'$ ) of PVA-borax hydrogel was also investigated corresponding to each pH solution as shown in Fig. S1b (Supporting information). Compared to the  $G'$  ( $6687.27 \pm 989.61$  Pa) of original hydrogel at  $pH \sim 7.6$ , it decreased obviously corresponding to each pH value ranged from 1.0 to 6.0. When treated by the pH solution higher than 6.0 ( $pH$  6.86 and  $pH$  7.6), the  $G'$  has no changes. It proved that PVA-borax hydrogel could undergo gel-sol transition when  $pH \leq 6.0$ . These rheological results were consistent with the optical observation in Fig. S1a. Furthermore, the sol state of PVA-

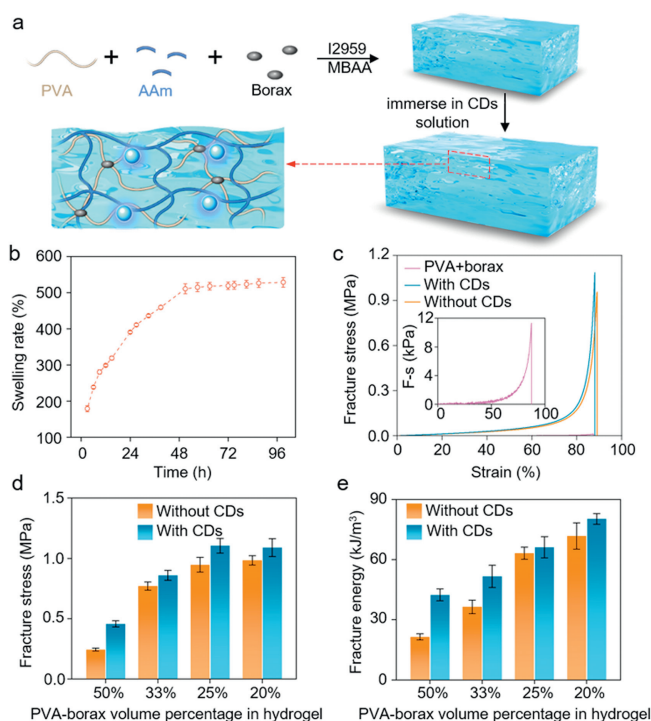


**Fig. 2.** Preparation and characterization of CDs-enhanced pH-responsive lubricating hydrogel. (a) Composition and preparation method of CPLH. (b) The swelling curve of CPLH (25% PVA-borax volume percentage). (c) The mechanical property of PVA-borax hydrogel, pH-responsive lubricating hydrogel without CDs and CPLH (25% PVA-borax volume percentage, with CDs). (d) The fracture stress of pH-responsive lubricating hydrogel with or without CDs. (e) The fracture energy of pH-responsive lubricating hydrogel with or without CDs.

borax in acid condition would transfer to gel state when  $pH \geq 8.5$ , which  $G'$  in sol state also increased to around 7000 Pa, correspondingly. As the gel-sol transition occurs, the surface viscosity of PVA-borax hydrogel decreased compared with original gel state when  $pH \leq 6.0$  (Fig. S1c in Supporting information). It can be attributed to the appearance of sol layer on the surface. But when  $pH = 6.86$  and 7.6, the viscosity was similar to the original gel state, because it could not occur gel-sol transition. When  $pH \geq 8.5$ , the viscosity on the hydrogel surface was similar with the value of original gel state (Fig. S1d in Supporting information). The original coefficient of friction (COF) of PVA-borax hydrogel was as high as 0.819–0.979 (Fig. S2a in Supporting information). When  $pH$  6.0 buffer solution was added on the hydrogel surface, the COF decreased to 0.030 because the PVA-borax hydrogel transformed to the sol state. The fracture stress of untreated PVA-borax hydrogel is 11.32 kPa and it decreased to 5.17 kPa after treated by  $pH$  6.0 buffer solution, because of the gel-sol transition (Fig. S2b in Supporting information). These results verified that the pH-responsiveness of PVA-borax in both mechanics and lubrication. As shown in Fig. S2c (Supporting information), the  $G'$  and  $G''$  of PVA-borax hydrogel exhibited well reversibility, the original  $G'$  was about 7.0 kPa. After treated by  $pH$  6.0 buffer solution, it sharply decreased to about 0.1 kPa. And treated by  $pH$  8.5 solution again, the  $G'$  would return back to about 7.0 kPa.

As shown in Fig. 2a, the prepared CDs-enhanced pH-responsive lubricating hydrogel was composed of CDs, PVA-borax and PAAm networks. A series of hydrogels were prepared by controlling the volume percentage of dynamic covalent bondings network (PVA-borax) in the hydrogel, which were 50%, 33%, 25% and 20%, respectively. In this study, CDs used in the hydrogel was synthesized by hydrothermal method of citric acid-ethylenediamine [31], which could be identified through UV, fluorescence and FTIR spec-

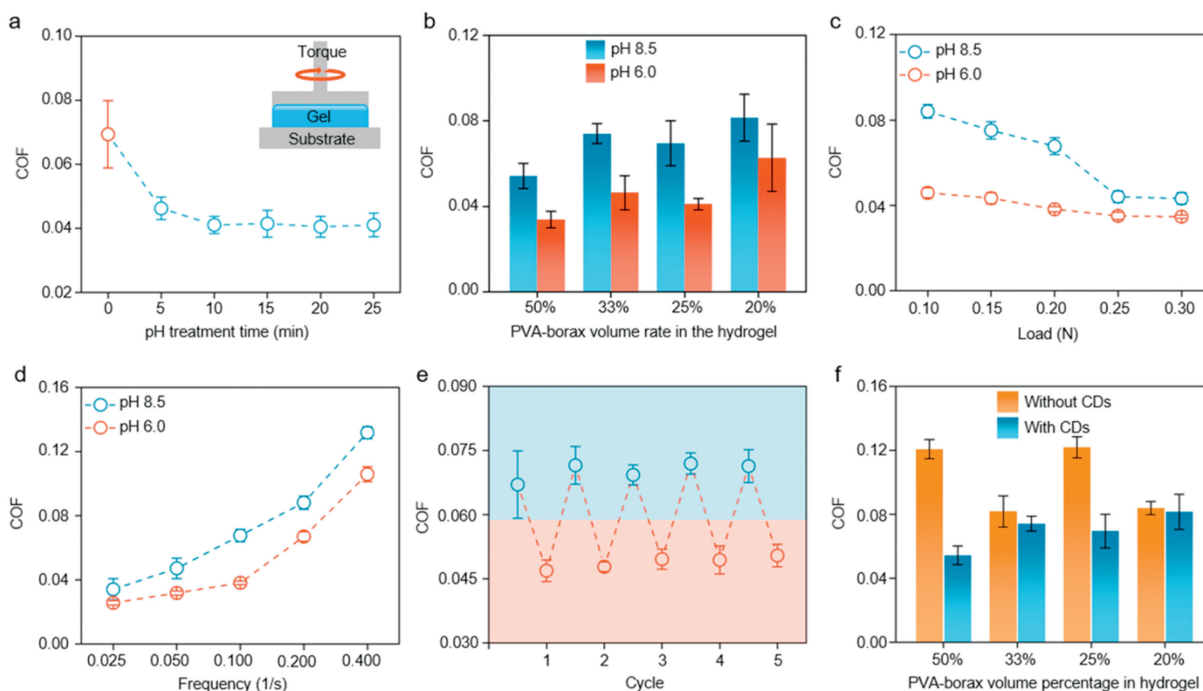


**Fig. 3.** Lubrication on the CDs-enhanced pH-responsive lubricating hydrogel. (a) The COF of CPLH (25% PVA-borax volume percentage) following pH treatment time from 0 to 25 min. (b) The COF of these CPLHs when treated by solution at pH 8.5 and 6.0. (c) The relationship between COF and load of 0.10, 0.15, 0.20, 0.25 and 0.30 N at pH 8.5 and 6.0. (d) The relationship between COF and frequency of 0.025, 0.050, 0.100, 0.200 and 0.400 1/s at pH 8.5 and 6.0. (e) The COF reversibility of CPLH in acidic (pH 6.0, orange) and basic (pH 8.5, blue) condition. (f) The COF of pH-responsive lubricating hydrogel with and without CDs introduction. Test sample in Figs. 3c-e was CPLH with 25% PVA-borax volume percentage. Friction test condition in Figs. 3a, b, e and f was load at 0.20 N, frequency at 0.100 1/s.

trum (Figs. S3a-c in Supporting information). The typical swelling curve of CPLH with 25% PVA-borax volume percentage as shown in Fig. 2b, the swelling equilibrium was achieved after about 60 h. All hydrogels used in this work were swelling completely. Firstly, the effect of CDs concentration in the pH-responsive lubricating hydrogel on the mechanical and lubrication properties was investigated as shown in Fig. S4 (Supporting information). In order to easily differentiate hydrogels in this work, the hydrogel without CDs is pH-responsive lubricating hydrogel, and the hydrogel with CDs is CDs-enhanced pH-responsive lubricating hydrogel (CPLH). In the experiment, the CDs concentration in the hydrogel was selected as 0.5, 1.0 and 2.0 mg/mL, the fracture stress of hydrogel with these three CDs concentrations were  $0.456 \pm 0.028$  MPa,  $0.456 \pm 0.025$  MPa and  $0.462 \pm 0.034$  MPa, respectively. They were higher than that without CDs introduction ( $0.243 \pm 0.011$  MPa) (Fig. S4a). Regarding the lubrication, the COF of the hydrogel with CDs concentration of 0.5, 1.0 and 2.0 mg/mL were  $0.051 \pm 0.013$ ,  $0.054 \pm 0.006$  and  $0.056 \pm 0.006$ , correspondingly. They were lower than the COF of the hydrogel without CDs introduction ( $0.121 \pm 0.006$ ) (Fig. S4b). Based on the above analysis, the introduction of CDs in the pH-responsive hydrogel would increase the mechanical property and decrease the COF. In addition, the selected CDs concentration in the experiment has little effect on mechanical and lubrication properties, so the CDs concentration in the hydrogel was chosen of 1.0 mg/mL. The fracture stress of CPLH with 25% PVA-borax volume percentage was about 1.087 MPa (Fig. 2c), which was much higher than those of PVA-borax hydrogel (11.324 kPa) and the hydrogel without CDs (0.958 MPa). The weak mechanical strength of PVA-borax hydrogel could be attributed to weak dynamic covalent bondings. Compared to the hydrogel without CDs, the mechanics of CPLH (with CDs) exhibited relative higher strength that could be ascribed to the possible principle of organic-inorganic composites and hydrogen bonding interaction [58,59]. The prepared citric acid-ethylenediamine CDs surface has a large number of amino and carboxyl groups, and can formed hydrogen bondings with the

network. Meanwhile, the CDs is rigid nanoparticles, it can be used as a filler dispersed uniformly in the pores of the hydrogel, and absorbing fracture energy under the action of external forces. As shown in Fig. 2d, the fracture stress of the prepared CPLHs was higher than those without CDs doping. For example, the fracture stress of hydrogel with 25% PVA-borax volume percentage increased from  $0.947 \pm 0.060$  MPa to  $1.104 \pm 0.061$  MPa. In addition, the fracture energy of the prepared hydrogels also increased from  $21.400 \pm 1.539$  kJ/m<sup>3</sup> to  $71.733 \pm 6.506$  kJ/m<sup>3</sup> (Fig. 2e) following the decreased dynamic covalent bondings percentage. For each percentage setpoint, the prepared CPLHs presented higher value than that hydrogels without CDs doping. It further verified that the introduction of CDs can improve the hydrogel mechanical property.

The tribological properties of the prepared hydrogel was shown in Fig. 3a. The original COF of CPLH (25% PVA-borax volume percentage) was  $0.069 \pm 0.011$ , which gradually decreased to  $0.041 \pm 0.003$  after treated by acidic solution of pH 6.0 for 10 min. It can be attributed that, when treated with pH 6.0 buffer solution, the formed boronic ester of PVA-borax in the hydrogel would disassembly, and a partial gel-sol transition occurred. Consequently, a sol layer composed of PVA, boracic acid and free CDs appeared on the hydrogel surface that results in the decrease of COF. Compared to these hydrogels, the COF of PAAm/PVA hydrogel without borax has not been influenced by pH 6.0 buffer solution (Fig. S5a in Supporting information). The COF of PAAm/PVA hydrogel remains stable following the pH treatment time. In addition, as water has strong effect on the surface lubrication, the COF of the hydrogel surface was analyzed when deionized water existed. There was no COF change on the hydrogel surface (Fig. S5b in Supporting information). The prepared CPLHs exhibited the pH responsiveness at pH of 8.5 and 6.0, which decreased from  $0.054 \pm 0.006$  to  $0.034 \pm 0.004$  of CPLH with 50% PVA-borax volume percentage,  $0.074 \pm 0.005$  to  $0.046 \pm 0.008$  of CPLH with 33% PVA-borax volume percentage,  $0.069 \pm 0.011$  to  $0.041 \pm 0.003$  of CPLH with 25% PVA-borax volume percentage,  $0.081 \pm 0.011$  to  $0.063 \pm 0.016$  of CPLH

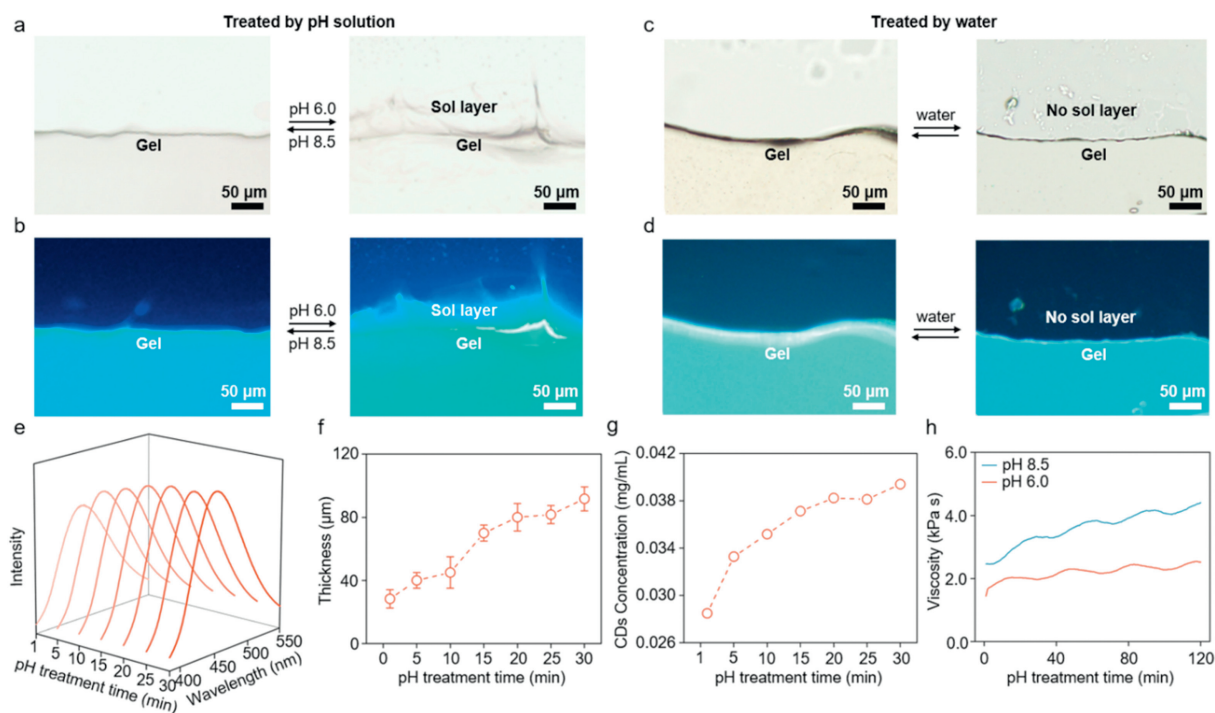


**Fig. 4.** Identification on the pH-responsiveness and the sol layer of the CDs-enhanced pH-responsive lubricating hydrogel. (a) The optical microscope photograph of the appearance of sol layer on hydrogel surface at pH 8.5 and 6.0. (b) The corresponding fluorescence microscope photograph of the appearance of sol layer. (c, d) The optical and fluorescence microscope photograph of CPLH treated with water at pH 7.4. (e) The relationship between fluorescence intensity of extracting solution and pH treatment time. (f) The relationship between thickness of sol layer and pH treatment time. (g) The relationship between exuded CDs concentration in the extracting solution and pH treatment time. (h) The surface viscosity on CPLH at pH 8.5 and 6.0. Test sample was CPLH with 25% PVA-borax volume percentage.

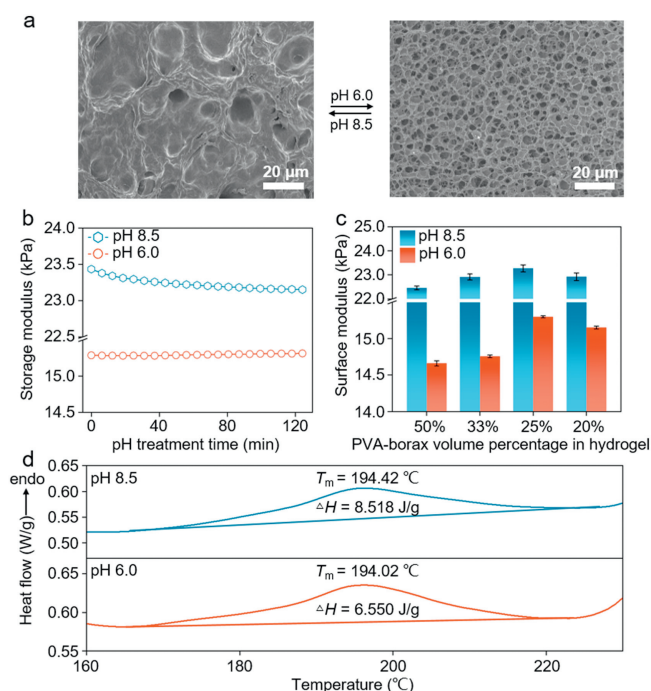


**Fig. 5.** The mechanical property of the CDs-enhanced pH-responsive lubricating hydrogel following pH. (a) The scanning electronic microscope of the hydrogel surface at pH 8.5 and 6.0. (b) The surface modulus of CPLH at pH 8.5 and 6.0. (c) The surface modulus on the hydrogel with controlled PVA percentage. (d) The differential scanning calorimetry of CPLH at pH 8.5 and 6.0. Test sample in Figs. 5a, b and d was CPLH with 25% PVA-borax volume percentage.

with 20% PVA-borax volume percentage, correspondingly (Fig. 3b). It can be seen that the CPLH with 50% PVA-borax volume percentage exhibited lowest COF among the prepared CPLHs, the fric-

tion behaviors in whole pH range was investigated in the experiment. The COF of the CPLH in the acidic range from 1.0 to 6.0 was around 0.033 (Fig. S6 in Supporting information). On the other hand, the COF in basic range from 7.6 to 14.0 was about 0.054. These COF results in the whole pH range was consistent with the tendency of the storage modulus  $G'$  and viscosity (Fig. S1b). When the acid-treated hydrogel was treated again with the buffer solution of pH  $\geq 8.5$ , the COF would return to its original state that was about 0.054.

As load and frequency are important factors for the tribology performance. Firstly, by adjusting the load from 0.10N to 0.30N and fixed frequency at 0.100 1/s, the COF of CPLH with 25% PVA-borax volume percentage decreases following the increasing of load. In the pH condition of 8.5 it decreased from  $0.084 \pm 0.003$  to  $0.043 \pm 0.003$ . For the condition at pH 6.0, the COF decreased from  $0.046 \pm 0.002$  to  $0.035 \pm 0.001$  (Fig. 3c). When control load is 0.30N, adjusting the frequency from 0.025 1/s to 0.400 1/s, the COF increased with frequency from  $0.034 \pm 0.007$  to  $0.132 \pm 0.004$  at pH 8.5. For the situation at pH 6.0, COF increased from  $0.026 \pm 0.001$  to  $0.106 \pm 0.005$  (Fig. 3d). PVA-borax hydrogel underwent a reversible gel-sol transition when treated with acidic and alkaline pH buffer solution, the reversibility of the COF was presented in Fig. 3e. In addition, the prepared CPLHs showed lower COF than those without CDs introduction (Fig. 3f). It confirmed that CDs introduction could improve hydrogel surface lubrication. Regarding to the hydrogel (with 50% PVA-borax volume percentage) without CDs introduction, the surface COF was  $0.121 \pm 0.006$ , and decreased gradually to  $0.107 \pm 0.007$  following to treatment time of pH 6.0 for 10 min (Fig. S7a in Supporting information). Moreover, this hydrogel without CDs introduction exhibited relative lower COF (0.107) in acidic range from 1.0 to 6.0, than those (0.121) in neutral and basic range from 8.5 to 14.0 as shown in Fig. S7b (Supporting information). These results proved that, first, the pH responsiveness was originated from the dynamic covalent

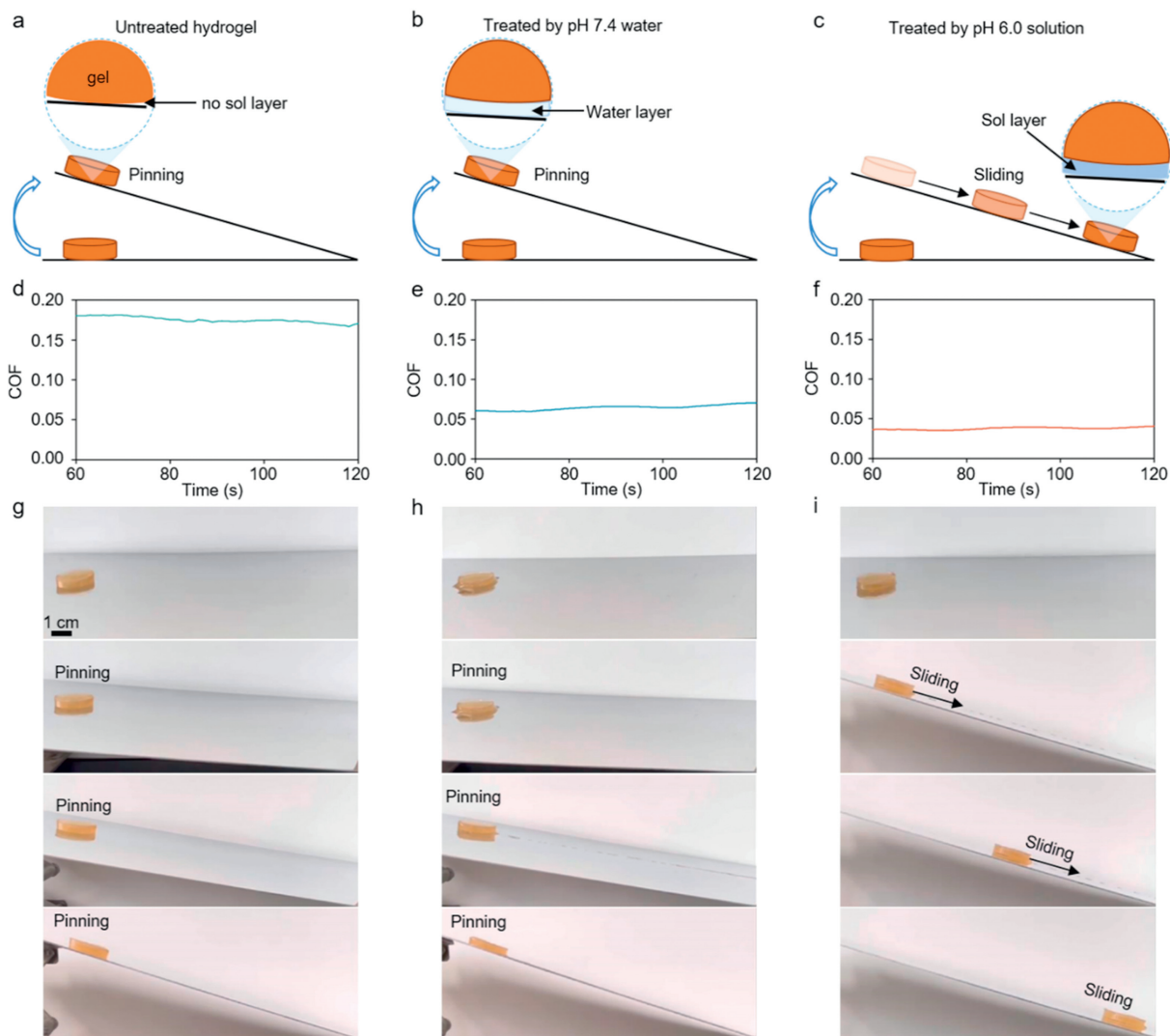


**Fig. 6.** The demonstration on the pH-responsive lubrication of the CDs-enhanced pH-responsive lubricating hydrogel. (a-c) Schematic diagram of the lubricating control of the no treated hydrogel, hydrogel treated by pH 7.4 water and treated by pH 6.0 solution. (d-f) The COF curves of the corresponding hydrogel. (g-i) The corresponding lubricating control photography. Demonstration sample was CPLH with 25% PVA-borax volume percentage.

bondings of PVA-borax in the hydrogel; secondary, the CDs could be benefit to the hydrogel lubrication.

To identify the appearance of a sol layer on the CDs-enhanced pH-responsive lubricating hydrogel surface after acidic treatment, a direct observation on the hydrogel surface (CPLH with 25% PVA-borax volume percentage) treated by buffer solution of pH 8.5 and 6.0 was shown in Fig. 4a. Compared to the hydrogel surface at pH 8.5, there was a sol layer observed on the surface after being treated by the buffer solution at pH 6.0. As CDs has blue fluorescence, one can observe a bright blue hydrogel and black background at pH 8.5 (Fig. 4b). After being treated by the buffer solution at pH 6.0, a wavy sol layer with blue fluorescence was found onto the hydrogel surface. To identifying the sol layer originate from the disassembly of PVA-borax dynamic covalent bondings at pH 6.0, a contrast experiment was introduced that the hydrogel surface was treated by deionized water at pH 7.4, as shown in Figs. 4c and d, there was no sol layer observed on the surface. It confirmed that the sol layer was derived from the disassembly of PVA-borax dynamic covalent bondings at pH 6.0, but not residual water layer after pH solution treatment.

The relationship between the thickness of the sol layer and the pH-responsive time was observed in quantity as shown in Fig. 4f,

the sol layer was generated at 1 min, and the thickness was about  $28.3 \pm 5.8 \mu\text{m}$ . With the increase of the treated time, the thickness of the sol layer increased gradually to  $91.7 \pm 7.6 \mu\text{m}$  at 30 min. Due to the fluorescence from CDs at 447 nm, the sol layer can be also analyzed by the fluorescence spectrum. In Fig. 4e, the extract on the hydrogel surface was obtained by rinsing the responsive CPLH with 25% PVA-borax volume percentage surface with 1 mL of deionized water. The fluorescence intensity increased with the pH treated time, indicating that there is more CDs appearing on the surface. Based on a standard calibration curve of CDs solution (Fig. S8 in Supporting information), the CDs concentration in the sol layer can be found that increased with the pH treated time from 0.029 mg/mL to 0.039 mg/mL (Fig. 4g). Furthermore, as the sol layer on the surface, the surface viscosity of CPLH with 25% PVA-borax volume percentage also changes correspondingly. As shown in Fig. 4h, the viscosity is about 3.828 kPa s at pH 8.5, and decreased to 2.215 kPa s at pH 6.0. The reduction of surface viscosity was attributed to the formation of the sol layer on the hydrogel surface. Compared to these, different viscosity solutions of PVA with CDs was drops on PAAm hydrogel substrates (Fig. S9 in Supporting information). The surface viscosity of PAAm hydrogel substrates was about 12.144 kPa s (0.10 1/s), and when water was dropped,

its surface viscosity decreased to 6.202 kPa s dramatically; When different concentration PVA (PVA1 means the concentration of PVA is 0.01%, PVA2 0.1%, PVA3 0.5%) with CDs solution (1 mg/mL) was dropped, the surface viscosity was decreasing with increasing concentration of PVA and CDs concentration, down to 4.732 kPa s. One can conclude that the surface viscosity of hydrogel will decrease when the sol layer is present on the hydrogel surface. For the other CPLHs, the surface viscosity exhibited the same tendency as shown in Fig. S10 (Supporting information).

As shown in Fig. 5a, the CPLH with 25% PVA-borax volume percentage surface showed occluded and anomalous micro-structures at pH 8.5, which is similar to the micro-structures of PVA-borax hydrogel (Fig. S11 in Supporting information). When the hydrogel surface was treated with pH 6.0 buffer solution, accompanying with the disassembly of PVA-borax dynamic covalent bondings in the hydrogel network, the surface structure transformed to microporous structures. The gel state PVA-borax network in the hydrogel underwent gel-sol transition, the sol state composed of PVA, boric acid and CDs wept out from the hydrogel network, therefore the hydrogel structures become porous and flexible. Consequently, the surface modulus of CPLH with 25% PVA-borax volume percentage decreased from 23.212 kPa at pH 8.5 to 15.295 kPa at pH 6.0 (Fig. 5b). The same tendency could be observed on prepared hydrogels (Fig. 5c). The differential scanning calorimetry (DSC) of CPLH with 25% PVA-borax volume percentage was characterized following the pH changes (Fig. 5d). As stronger bonding interactions in network indicates higher endothermic enthalpy ( $\Delta H$ ). For the hydrogel at pH 8.5, the dynamic covalent bondings of PVA and borax was binding state that  $\Delta H$  was 8.518 J/g. After treated by the solution with pH 6.0, the  $\Delta H$  reduced to 6.550 J/g. It meant that the disassembly of PVA-borax brought weaker bonding interactions than the assembled state at pH 8.5. It consistent with the SEM observation and rheological results in Figs. 5a and b.

For demonstrate the pH-responsive lubrication of the hydrogel, the CPLH with 25% PVA-borax volume percentage was placed on a stainless-steel substrate (Fig. 6 and movie S1 in Supporting information). In Figs. 6a, d and g, the untreated CPLH was pinning on the substrate due to the high static COF of 0.170. With treated by pH 7.4 water (Figs. 6b, e and h), the COF of the CPLH decreases significantly to 0.064, but similarly, the CPLH is still pinning on the substrate. When the hydrogel was treated by pH 6.0 solution (Figs. 6c, f and i), there was a sol layer formed between CPLH and substrate. The COF of the hydrogel further decreased to 0.038 and slid down.

In summary, we reported a CDs-enhanced hydrogel composed of PVA-borax dynamic covalent bondings and covalent polymer network. In acidic pH environment ranged from 1.0 to 6.0, the PVA-borax network in the hydrogel will disassembly and form the sol lubricating layer on the hydrogel surface. The coefficient of friction on hydrogel surface changes from  $0.069 \pm 0.011$  to  $0.041 \pm 0.003$  reversibility. The introduction of CDs improves not only the lubricating capability but also the mechanical property of the hydrogel. Moreover, the fluorescence properties of the CDs endow the sol lubricating layer with unique observability, which blue sol layer could be observed under fluorescence microscopy. This study provides a promising idea for designing pH-responsive hydrogels for potential applications on soft actuator or robot, the future work can be foreseen to develop durable and more sensitive lubricating hydrogel.

#### Declaration of competing interest

The authors declare that they have no known competing financial interests or personal relationships that could have appeared to influence the work reported in this paper.

#### Acknowledgment

This research was supported by the National Natural Science Foundation of China (No. 22175075).

#### Supplementary materials

Supplementary material associated with this article can be found, in the online version, at doi:10.1016/j.ccllet.2023.109297.

#### References

- [1] S. Choi, K.Y. Lee, S.L. Kim, et al., *Nat. Mater.* 22 (2023) 1039–1046.
- [2] N. Xu, J. Wang, L. Liu, C. Gong, *Chin. Chem. Lett.* (2023), doi:10.1016/j.ccllet.2023.109225.
- [3] S.J. Jeon, A.W. Hauser, R.C. Hayward, *Acc. Chem. Res.* 50 (2017) 161–169.
- [4] C. Löwenberg, M. Balk, C. Wischke, et al., *Acc. Chem. Res.* 50 (2017) 723–732.
- [5] P. Chen, C. Yu, J. Chen, et al., *Chin. Chem. Lett.* 34 (2023) 108627.
- [6] S. Wang, M.W. Urban, *Nat. Rev. Mater.* 5 (2020) 562–583.
- [7] T. Zhou, H. Yuk, F. Hu, et al., *Nat. Mater.* 22 (2023) 895–902.
- [8] M. Lin, H. Hu, S. Zhou, S. Xu, *Nat. Rev. Mater.* 7 (2022) 850–869.
- [9] M. Li, A. Pal, A. Aghakhani, et al., *Nat. Rev. Mater.* 7 (2022) 235–249.
- [10] G. Fusi, D. Del Giudice, O. Skarsetz, et al., *Adv. Mater.* 35 (2023) 2209870.
- [11] V. Yesilyurt, M.J. Webber, E.A. Appel, et al., *Adv. Mater.* 28 (2016) 86–91.
- [12] S.H. Hong, M. Shin, E. Park, et al., *Adv. Funct. Mater.* 30 (2020) 1908497.
- [13] Y. Hu, Z. Wang, D. Jin, et al., *Adv. Funct. Mater.* 30 (2020) 1907377.
- [14] B. Narupai, P.T. Smith, A. Nelson, *Adv. Funct. Mater.* 31 (2021) 2011012.
- [15] L. Sherwood, *Human Physiology: From Cells to Systems*, 7<sup>th</sup> Ed., Brooks/Cole, New York, 2010.
- [16] A.L. Chau, P.T. Getty, A.R. Rhode, et al., *Front. Chem.* 10 (2022) 891519.
- [17] Y. Hu, S. Gao, H. Lu, J.Y. Ying, *J. Am. Chem. Soc.* 144 (2022) 5461–5470.
- [18] X. Zhang, J. Wang, H. Jin, et al., *J. Am. Chem. Soc.* 140 (2018) 3186–3189.
- [19] X. Zhang, K. Shi, X. Yang, et al., *CCS Chem.* 5 (2023) 2482–2496.
- [20] J. Wang, X. Zhang, S. Zhang, et al., *Matter* 4 (2021) 675–687.
- [21] N. Li, C. Liu, W. Chen, J. Agric. Food. Chem. 67 (2019) 746–752.
- [22] H.F. Mahjoub, M. Zammali, C. Abbes, T. Othman, *J. Mol. Liq.* 291 (2019) 111272.
- [23] C. Wang, Z. Shen, P. Hu, et al., *J. Sol-Gel Sci. Technol.* 101 (2022) 103–113.
- [24] Y. Guan, Y. Zhang, *Chem. Soc. Rev.* 42 (2013) 8106–8121.
- [25] W.L.A. Brooks, B.S. Sumerlin, *Chem. Rev.* 116 (2016) 1375–1397.
- [26] S. Naaz, S. Poddar, S.P. Bayen, et al., *Sens. Actuators B: Chem.* 255 (2018) 332–340.
- [27] X. Yang, X. Li, B. Wang, et al., *Chin. Chem. Lett.* 33 (2022) 613–625.
- [28] M. Fang, B. Wang, X. Qu, et al., *Chin. Chem. Lett.* 35 (2024) 108423.
- [29] B. Wang, G.I.N. Waterhouse, S. Lu, *Trends Chem.* 5 (2023) 76–87.
- [30] S. Zhu, J. Zhang, C. Qiao, et al., *Chem. Commun.* 47 (2011) 6858–6860.
- [31] S. Zhu, Q. Meng, L. Wang, et al., *Angew. Chem. Int. Ed.* 52 (2013) 3953–3957.
- [32] T. Feng, Q. Zeng, S. Lu, et al., *ACS Photonics* 5 (2018) 502–510.
- [33] J. Shao, S. Zhu, H. Liu, et al., *Adv. Sci.* 4 (2017) 1700395.
- [34] S. Tao, S. Lu, Y. Geng, et al., *Angew. Chem. Int. Ed.* 57 (2018) 2393–2398.
- [35] J. Liu, Y. Geng, D. Li, et al., *Adv. Mater.* 32 (2020) 1906641.
- [36] C. Zheng, S. Tao, B. Yang, *Small Struct.* 4 (2023) 2200327.
- [37] C. He, S. E. H. Yan, X. Li, *Chin. Chem. Lett.* 32 (2021) 2693–2714.
- [38] W. Tang, Z. Zhang, Y. Li, *J. Mater. Sci.* 56 (2021) 12061–12092.
- [39] W. Zhang, T. Li, R. An, et al., *Friction* 10 (2022) 1751–1771.
- [40] M. Han, S. Zhu, S. Lu, et al., *Nano Today* 19 (2018) 201–218.
- [41] Y. Zhao, Q. Zeng, Y. Yu, et al., *Mater. Horiz.* 7 (2020) 2719–2725.
- [42] T. Feng, G. Yu, S. Tao, et al., *J. Mater. Chem. A* 8 (2020) 9638–9645.
- [43] J. Yu, H. Song, X. Li, et al., *Adv. Funct. Mater.* 31 (2021) 2107196.
- [44] H. Wu, S. Lu, B. Yang, *Acc. Mater. Res.* 3 (2022) 319–330.
- [45] Y. Yu, Q. Zeng, S. Tao, et al., *Adv. Sci.* (2023) 2207621.
- [46] X. Xu, K. Zhang, L. Zhao, et al., *ACS Appl. Mater. Interfaces* 8 (2016) 32706–32716.
- [47] K.K. Liu, S.Y. Song, L.Z. Sui, et al., *Adv. Sci.* 6 (2019) 1900766.
- [48] L. Jiang, H. Ding, M. Xu, et al., *Small* 16 (2020) 2000680.
- [49] D. Li, L. Lin, Y. Fan, et al., *Bioact. Mater.* 6 (2021) 729–739.
- [50] T. Han, Y. Wang, S. Ma, et al., *Adv. Sci.* 9 (2022) 2203474.
- [51] J. Ge, Q. Jia, W. Liu, et al., *Adv. Mater.* 27 (2015) 4169–4177.
- [52] Q. Jia, J. Ge, W. Liu, et al., *Adv. Mater.* 30 (2018) 1706090.
- [53] L. Hou, D. Chen, R. Wang, et al., *Angew. Chem. Int. Ed.* 60 (2021) 6581–6592.
- [54] W. Bing, H. Sun, Z. Yan, et al., *Small* 12 (2016) 4713–4718.
- [55] J. Liu, S. Lu, Q. Tang, et al., *Nanoscale* 9 (2017) 7135–7142.
- [56] H.J. Jian, R.S. Wu, T.Y. Lin, et al., *ACS Nano* 11 (2017) 6703–6716.
- [57] B. Geng, P. Li, F. Fang, et al., *Carbon* 184 (2021) 375–385.
- [58] X. Sun, Z. Qin, L. Ye, et al., *Chem. Eng. J.* 382 (2020) 122832.
- [59] X. Meng, Y. Qiao, C. Do, et al., *Adv. Mater.* 34 (2022) 2108243.